

# Journal of Mechanics of Materials and Structures

**BUCKLING AND POSTBUCKLING BEHAVIOR OF FUNCTIONALLY GRADED  
TIMOSHENKO MICROBEAMS BASED ON THE STRAIN GRADIENT THEORY**

Reza Ansari, Mostafa Faghieh Shojaei, Vahid Mohammadi, Raheb Gholami  
and Mohammad Ali Darabi

Volume 7, No. 10

December 2012



# BUCKLING AND POSTBUCKLING BEHAVIOR OF FUNCTIONALLY GRADED TIMOSHENKO MICROBEAMS BASED ON THE STRAIN GRADIENT THEORY

REZA ANSARI, MOSTAFA FAGHIH SHOJAEI, VAHID MOHAMMADI,  
RAHEB GHOLAMI AND MOHAMMAD ALI DARABI

Presented herein is a comprehensive study on the buckling and postbuckling analysis of microbeams made of functionally graded materials (FGMs) based on the modified strain gradient theory. The present model is developed in the skeleton of the Timoshenko beam theory and the von Karman geometric non-linearity, and enables one to consider size effects through introducing material length scale parameters. Also, the current model can be reduced to the modified couple stress and classical models if two or all material length scale parameters are set equal to zero, respectively. Utilizing a power law function, the volume fraction of the ceramic and metal phases of the functionally graded microbeam is expressed. The stability equations and corresponding boundary conditions are derived using Hamilton's principle and then solved through the generalized differential quadrature (GDQ) method in conjunction with a direct approach without linearization. The effects of the length scale parameter, slenderness ratio, material gradient index and boundary conditions on the buckling and postbuckling behavior of microbeams are carefully studied. Furthermore, the non-dimensional critical axial load of microbeams predicted by modified strain gradient and classical theories for the first three postbuckling modes is investigated and it is observed that the classical theory underestimates the non-dimensional critical axial load, especially at higher postbuckling modes. In addition, the influence of imperfections on the deflection of microbeams in prebuckled and postbuckled states is discussed.

## 1. Introduction

Microstructures made of FGMs are becoming hot research areas, since they pave the way for achieving highly sensitive and most desired micro-electromechanical systems [Hasanyan et al. 2008; Witvrouw and Mehta 2005; Fu et al. 2004].

As the size-dependent deformation behavior is detected in the micro-torsion and micro-bending experiments of microbeams, the size effects must be incorporated in the study of FGM microstructures. The conventional continuum mechanics is not able to capture size effects; hence, developing size-dependent elasticity theories has become an important issue. In this regard, several non-classical continuum theories such as the strain gradient elasticity, couple stress elasticity, nonlocal elasticity and the surface elasticity have been proposed [Aifantis 1999; Mindlin and Tiersten 1962; Eringen 1972; Gurtin et al. 1998]. The two first size-dependent theories encompass some higher-order stress constituents in addition to the classical stresses.

---

*Keywords:* FGM microbeam, generalized differential quadrature method, strain gradient theory, mechanical buckling, postbuckling, Timoshenko beam theory.

One type of the higher-order continuum theories reported in [Mindlin and Tiersten 1962](#); [Koiter 1964](#); [Toupin 1962](#); [1964](#)] is the couple stress theory which includes two material length scale parameters in addition to classical material constants for isotropic elastic materials. These two material length scale parameters are in relation to the underlying microstructure of material and are so complicated to determine. [Yang et al. \[2002\]](#) proposed the modified couple stress theory (MCST) and facilitated applying couple stress theory by considering only one material length scale parameter beside two classical material constants. A variational formulation for the MCST was also presented by [Park and Gao \[2008\]](#). This theory has been extensively used to interpret size effects on the vibrational, bending and buckling behavior of microstructures [[Ma et al. 2008](#); [2010](#); [2011](#); [Tsiatas 2009](#); [Xia et al. 2010](#); [Park and Gao 2006](#)].

The strain gradient theory proposed by [Fleck and Hutchinson \[1993\]](#) is the extension of Mindlin's formulation [[Mindlin 1964](#); [1965](#); [Mindlin and Eshel 1968](#)] which considers only the first derivative of the strain tensor. In comparison with the couple stress theory, this theory comprises some higher-order stress constituents beside the classical and couple stresses. [Lam et al. \[2003\]](#) introduced the modified strain gradient theory (MSGT) through considering three higher-order material constants related to dilatation gradient, deviatoric gradient and symmetric rotation gradient tensors. It is noted that the MSGT is also a simplified version of the Mindlin's general theory [[Mindlin 1964](#); [1965](#); [Mindlin and Eshel 1968](#)] which can be developed by omitting the second-order derivatives of the strain components in the elastic strain energy. Numerous studies have been accomplished to investigate the size-dependent static bending and vibrational analysis of microstructures based on the MSGT. The static deformation and vibrational behavior of an Euler–Bernoulli microbeam was studied by [Kong et al. \[2009\]](#) using the MSGT. [Wang et al. \[2012\]](#) developed a micro-scaled Timoshenko beam model based on the MSGT and Hamilton's principle. They also studied the static bending and free vibration of a simply-supported Timoshenko microbeam. In another work, [Kahrobaian et al. \[2011\]](#), based on the MSGT, proposed a nonlinear size-dependent Euler–Bernoulli beam model and studied the nonlinear size-dependent static bending of a hinged-hinged microbeam. In a recent study, based on the MSGT, [Ansari et al. \[2012a\]](#) developed a nonlinear size-dependent Timoshenko microbeam model and examined the influences of geometric parameters, Poisson's ratio and material length scale parameters on the vibrational behavior of microbeams.

A literature review shows that the majority of studies on microstructures are concerned with the homogeneous materials. However, in recent years, several efforts have been tended to study the size-dependent mechanical behavior of microstructures made of FGMs [[Asghari et al. 2010](#); [2011](#); [Reddy and Jinseok 2012](#); [Mirzavand and Eslami 2011](#); [Ke et al. 2012](#); [Mohammadi-Alasti et al. 2011](#); [Ke and Wang 2011](#); [Ansari et al. 2012b](#); [2011](#)]. In this direction, utilizing the MCST, [Asghari et al. \[2010\]](#) studied the static and vibrational behavior of Euler–Bernoulli FGM microbeams. It was observed that when the ratio of the beam's characteristic size to the material length scale parameter is low, the results obtained by the MCST have a significant difference with those obtained by the classical theory (CT). [Ke and Wang \[2011\]](#) investigated size-dependent dynamic stability of FGM microbeams based on the MCST and Timoshenko beam theory. They found that when the thickness of beam is equal to the material length scale parameter, the size effect on the dynamic stability characteristics is prominent. [Ansari et al. \[2012b\]](#) investigated the nonlinear free vibration behavior of FGM microbeams based on the MSGT and the Timoshenko beam theory. They measured the influences of important parameters on the vibrational response of the microbeams.

In this paper, based on the MSGT, the buckling and postbuckling of FGM microbeams have been studied. To this end, the volume fraction of the ceramic and metal phases of FGM microbeams is expressed by using the power law function. In the framework of nonlinear Timoshenko beam theory, the stability equations and associated boundary conditions are derived employing Hamilton's principle. Then, the higher-order governing differential equations are discretized along with three different boundary conditions by using the GDQ method in conjunction with a direct approach without linearization. The current article provides an accurate insight into the effects of length scale parameter, slenderness ratio, material gradient index, and boundary conditions on the buckling and postbuckling behavior of FGM microbeams. The present model explicitly considers the net effect of imperfections of FGM microbeams which is owing to fabrication defects, geometric irregularities, and non-ideal loading. Recognizing the influence of imperfections is an important matter, since imperfections in structures are inescapable and may lead to considerable variations in the stability response. By considering imperfections, instead of sudden bifurcation at a critical axial load, the microbeams show a slight out-of-plane deflection from the prebuckled state to a postbuckled one.

## 2. Modified strain gradient theory

Based on the modified strain gradient theory of Lam et al. [2003], the stored strain energy  $U_m$  in a continuum constructed by a linear elastic material occupying region  $\Omega$  undergoing infinitesimal deformations is given as

$$U_m = \frac{1}{2} \int_{\Omega} (\sigma_{ij} \epsilon_{ij} + p_i \gamma_i + \tau_{ijk}^{(1)} \eta_{ijk}^{(1)} + m_{ij}^s \chi_{ij}^s) dv, \quad (1a)$$

$$\epsilon_{ij} = \frac{1}{2} (u_{i,j} + u_{j,i}), \quad (1b)$$

$$\gamma_i = \epsilon_{mm,i}, \quad (1c)$$

$$\eta_{ijk}^{(1)} = \eta_{ijk}^{(1)} = \eta_{ijk}^s - \frac{1}{5} (\delta_{ij} \eta_{mmk}^s + \delta_{jk} \eta_{mmi}^s + \delta_{ki} \eta_{mmj}^s), \quad \eta_{ijk}^s = \frac{1}{3} (\epsilon_{jk,i} + \epsilon_{ki,j} + \epsilon_{ij,k}), \quad (1d)$$

$$\chi_{ij}^s = \frac{1}{2} (\theta_{i,j} + \theta_{j,i}), \quad \theta_i = \frac{1}{2} (\text{curl}(u))_i \quad (1e)$$

where  $\epsilon_{ij}$  denotes the strain tensor and  $u_i$  is the components of displacement vector  $u$ . Also,  $\gamma_i$ ,  $\eta_{ijk}^{(1)}$ ,  $\chi_{ij}^s$  are dilatation gradient, deviatoric stretch gradient, and symmetric rotation gradient tensors, respectively [Lam et al. 2003].  $\theta_i$  stands for the infinitesimal rotation vector  $\theta$ , and  $\delta$  is the Kronecker delta.

The constitutive equations corresponding to a linear isotropic elastic material expressed by kinematic parameters effective on the strain energy density are [Lam et al. 2003; Timoshenko and Goodier 1970]

$$\sigma_{ij} = \lambda \text{tr}(\epsilon) \delta_{ij} + 2\mu \epsilon_{ij}, \quad p_i = 2\mu l_0^2 \gamma_i, \quad \tau_{ijk}^{(1)} = 2\mu l_1^2 \eta_{ijk}^{(1)}, \quad m_{ij}^s = 2\mu l_2^2 \chi_{ij}^s \quad (2)$$

in which  $\mathbf{p}$ ,  $\boldsymbol{\tau}^{(1)}$ , and  $\mathbf{m}^s$  present the higher-order stresses. Also,  $l_0$ ,  $l_1$ ,  $l_2$  stand for three independent material length scale parameters related to the dilatation gradients, deviatoric stretch gradients and symmetric rotation gradients, respectively. Also, in the constitutive equation of the classical stress,  $\lambda$  and  $\mu$  are two classical material constants of bulk and shear modules, respectively, and are given as [Timoshenko and Goodier 1970; Ke et al. 2010]

$$\lambda = \frac{E\nu}{(1+\nu)(1-2\nu)}, \quad \mu = \frac{E}{2(1+\nu)}. \quad (3)$$

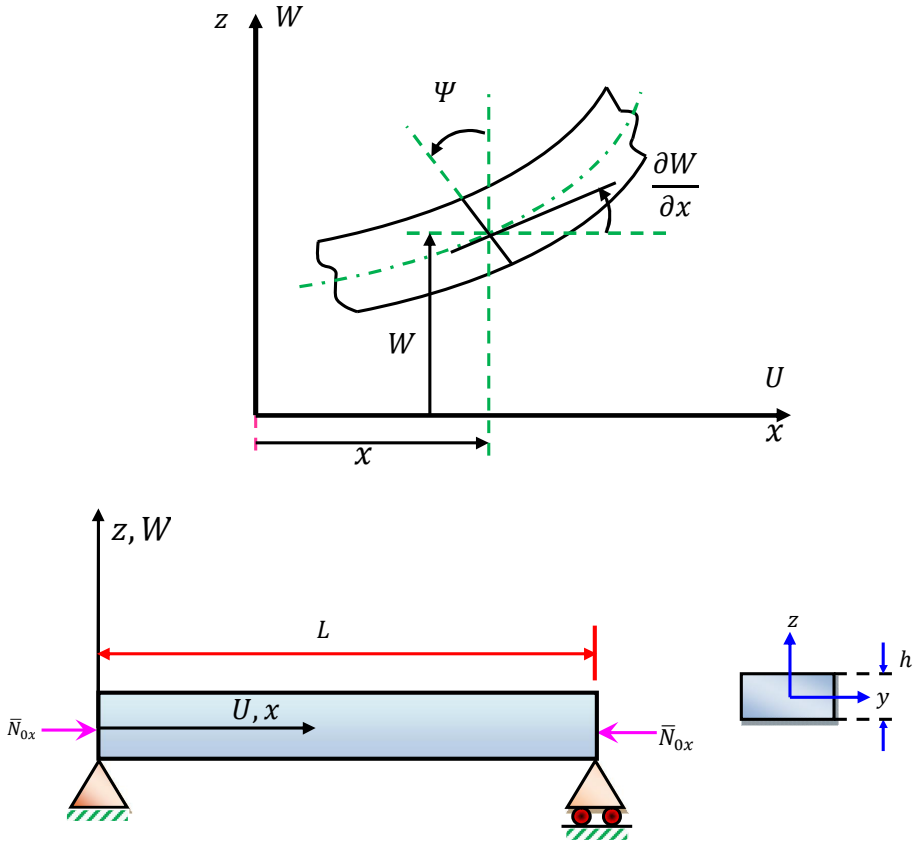


**Figure 1.** Schematic of a Timoshenko beam: kinematic parameters, coordinate system, geometry and loading.

Accordingly, the theory of [Lam et al. 2003] encompasses higher-order stresses beside the classical stress. These tensors are specified by three independent material length scale parameters and two classical material constants.

### 3. Material properties of FGM microbeams

As shown in Figure 1, consider a FGM microbeam made of a mixture of ceramic and metal with length  $L$  and thickness  $h$  undergoing an axial compressive load  $\bar{N}_{0x}$ . Also, the kinematic parameters and geometry and loading are demonstrated in this figure. The materials at bottom surface ( $z = -h/2$ ) and top surface ( $z = h/2$ ) of the microbeam are supposed to be metal-rich and ceramic-rich, respectively.

Effective material characteristics of the FGM microbeam such as Young’s modulus ( $E$ ) and Poisson’s ratio ( $\nu$ ) can be achieved as the following relations

$$E(z) = (E_c - E_m)V_f(z) + E_m, \tag{4}$$

$$\nu(z) = (\nu_c - \nu_m)V_f(z) + \nu_m, \tag{5}$$

where the subscripts  $m$  and  $c$  signify metal and ceramic phases, respectively. Amongst the different

existing functions to describe the variation of the volume fractions of constituents, herein a simple power law function is used to explain the volume fraction of the ceramic and metal phases as (see [Fares et al. 2009])

$$V_f(z) = \left(\frac{1}{2} + \frac{z}{h}\right)^k, \quad (6)$$

where  $k$  represents the power law index.

#### 4. Mathematical formulation of stability equations and associated boundary conditions

Based on the Timoshenko beam formulation, by introducing  $U(x)$ ,  $W(x)$ ,  $W_s(x)$  and  $\Psi(x)$  as the axial displacement of the center of sections, lateral deflection of the beam, lateral pre-deflection owing to imperfection, and the rotation angle of the cross section with respect to the vertical direction, the kinematics of microbeams are given as

$$u_1 = U(x) - z\Psi(x), \quad u_2 = 0, \quad u_3 = W(x) - W_s(x). \quad (7)$$

It is noteworthy to mention that in this study the net imperfection is treated as a pre-deflection of microbeam in unloaded state. By considering a Timoshenko microbeam under tiny slopes after deflection and possible finite transverse deflection  $W$ , the nonlinear strain-displacement relations are approximated by the von Karman relation as

$$\epsilon_{11} = \frac{du_1}{dx} + \frac{1}{2} \left[ \left( \frac{dW}{dx} \right)^2 - \left( \frac{dW_s}{dx} \right)^2 \right] = \frac{dU}{dx} - z \frac{d\Psi}{dx} + \frac{1}{2} \left[ \left( \frac{dW}{dx} \right)^2 - \left( \frac{dW_s}{dx} \right)^2 \right], \quad \epsilon_{13} = \frac{1}{2} \left( \frac{dW}{dx} - \frac{dW_s}{dx} - \Psi \right). \quad (8)$$

Also, the non-zero constituents of  $\theta$ ,  $\chi^s$ ,  $\gamma$  and  $\eta^{(1)}$  can be obtained through introducing (7) and (8) into (1c)–(1e) as

$$\theta_2 = -\frac{1}{2} \left( \Psi + \frac{dW}{dx} - \frac{dW_s}{dx} \right), \quad (9a)$$

$$\chi_{12}^s = \chi_{21}^s = -\frac{1}{4} \left( \frac{d\Psi}{dx} + \frac{d^2W}{dx^2} - \frac{d^2W_s}{dx^2} \right), \quad (9b)$$

$$\gamma_1 = \frac{d^2U}{dx^2} - z \frac{d^2\Psi}{dx^2} + \frac{dW}{dx} \cdot \frac{d^2W}{dx^2} - \frac{dW_s}{dx} \cdot \frac{d^2W_s}{dx^2}, \quad \gamma_3 = -\frac{d\Psi}{dx}, \quad (9c)$$

$$\eta_{111}^{(1)} = \frac{2}{5} \left( \frac{d^2U}{dx^2} - z \frac{d^2\Psi}{dx^2} + \frac{dW}{dx} \cdot \frac{d^2W}{dx^2} - \frac{dW_s}{dx} \cdot \frac{d^2W_s}{dx^2} \right), \quad \eta_{333}^{(1)} = -\frac{1}{5} \left( \frac{d^2W}{dx^2} - \frac{d^2W_s}{dx^2} - 2 \frac{d\Psi}{dx} \right),$$

$$\eta_{113}^{(1)} = \eta_{311}^{(1)} = \eta_{131}^{(1)} = \frac{4}{15} \left( \frac{d^2W}{dx^2} - \frac{d^2W_s}{dx^2} - 2 \frac{d\Psi}{dx} \right), \quad (9d)$$

$$\eta_{223}^{(1)} = \eta_{322}^{(1)} = \eta_{232}^{(1)} = -\frac{1}{15} \left( \frac{d^2W}{dx^2} - \frac{d^2W_s}{dx^2} - 2 \frac{d\Psi}{dx} \right),$$

$$\eta_{221}^{(1)} = \eta_{212}^{(1)} = \eta_{122}^{(1)} = \eta_{313}^{(1)} = \eta_{133}^{(1)} = \eta_{331}^{(1)} = -\frac{1}{5} \left( \frac{d^2U}{dx^2} - z \frac{d^2\Psi}{dx^2} + \frac{dW}{dx} \cdot \frac{d^2W}{dx^2} - \frac{dW_s}{dx} \cdot \frac{d^2W_s}{dx^2} \right).$$

Finally, by inserting (8) and (9) into (2), the major constituents of the symmetric section of the stress tensor and nonzero constituents of the higher-order stresses are achieved. The strain energy due to the

variation of the classical and higher order stresses with respect to the initial configuration  $\Pi_s$  can be written as

$$\begin{aligned} \Pi_s = \frac{1}{2} \int_0^L \left\{ N_1 \left( \frac{dU}{dx} + \frac{1}{2} \left[ \left( \frac{dW}{dx} \right)^2 - \left( \frac{dW_s}{dx} \right)^2 \right] \right) - M_1 \left( \frac{d\Psi}{dx} \right) + Q_1 \left( \frac{dW}{dx} - \frac{dW_s}{dx} - \Psi \right) - P_3 \left( \frac{d\Psi}{dx} \right) \right. \\ \left. + (P_1 + T_{111}^\tau) \left( \frac{d^2U}{dx^2} + \frac{dW}{dx} \cdot \frac{d^2W}{dx^2} - \frac{dW_s}{dx} \cdot \frac{d^2W_s}{dx^2} \right) - (M_1^p + M_{111}^\tau) \left( \frac{d^2\Psi}{dx^2} \right) \right. \\ \left. - \frac{4}{3} T_{333}^\tau \left( \frac{d^2W}{dx^2} - \frac{d^2W_s}{dx^2} - 2 \frac{d\Psi}{dx} \right) - \frac{Y_{12}}{2} \left( \frac{d\Psi}{dx} + \frac{d^2W}{dx^2} - \frac{d^2W_s}{dx^2} \right) \right\} dx, \quad (10) \end{aligned}$$

in which the normal resultant force  $N_1$ , shear force  $Q_1$ , bending moment  $M_1$ , couple moment  $Y_{12}$  and other higher-order resultants force and higher order moments in a section attributable to higher-order stresses acting on the section are introduced as follows:

$$N_1 = \int_A \sigma_{11} dA = A_{11} \left( \frac{dU}{dx} + \frac{1}{2} \left[ \left( \frac{dW}{dx} \right)^2 - \left( \frac{dW_s}{dx} \right)^2 \right] \right) - B_{11} \frac{d\Psi}{dx},$$

$$M_1 = \int_A \sigma_{11} z dA = B_{11} \left( \frac{dU}{dx} + \frac{1}{2} \left[ \left( \frac{dW}{dx} \right)^2 - \left( \frac{dW_s}{dx} \right)^2 \right] \right) - D_{11} \frac{d\Psi}{dx}, \quad (11a)$$

$$Q_1 = \int_A \sigma_{13} dA = k_s A_{55} \left( \frac{dW}{dx} - \frac{dW_s}{dx} - \Psi \right), \quad Y_{12} = \int_A m_{12}^s dA = -\frac{l_2^2}{2} A_{55} \left( \frac{d\Psi}{dx} + \frac{d^2W}{dx^2} - \frac{d^2W_s}{dx^2} \right),$$

$$P_1 = \int_A p_1 dA = 2l_0^2 \left( A_{55} \left[ \frac{d^2U}{dx^2} + \frac{dW}{dx} \cdot \frac{d^2W}{dx^2} - \frac{dW_s}{dx} \cdot \frac{d^2W_s}{dx^2} \right] - B_{55} \frac{d^2\Psi}{dx^2} \right),$$

$$P_3 = \int_A p_3 dA = -2A_{55} l_0^2 \frac{d\Psi}{dx}, \quad (11b)$$

$$T_{111}^\tau = \int_A \tau_{111}^{(1)} dA = \frac{4l_1^2}{5} \left( A_{55} \left[ \frac{d^2U}{dx^2} + \frac{dW}{dx} \cdot \frac{d^2W}{dx^2} - \frac{dW_s}{dx} \cdot \frac{d^2W_s}{dx^2} \right] - B_{55} \frac{d^2\Psi}{dx^2} \right), \quad (11c)$$

$$T_{333}^\tau = \int_A \tau_{333}^{(1)} dA = -\frac{2l_1^2}{5} A_{55} \left( \frac{d^2W}{dx^2} - \frac{d^2W_s}{dx^2} - 2 \frac{d\Psi}{dx} \right), \quad (11d)$$

$$M_1^p = \int_A p_1 z dA = 2l_0^2 \left( B_{55} \left[ \frac{d^2U}{dx^2} + \frac{dW}{dx} \cdot \frac{d^2W}{dx^2} - \frac{dW_s}{dx} \cdot \frac{d^2W_s}{dx^2} \right] - D_{55} \frac{d^2\Psi}{dx^2} \right), \quad (11e)$$

$$M_{111}^\tau = \int_A \tau_{111}^{(1)} z dA = \frac{4l_1^2}{5} \left( B_{55} \left[ \frac{d^2U}{dx^2} + \frac{dW}{dx} \cdot \frac{d^2W}{dx^2} - \frac{dW_s}{dx} \cdot \frac{d^2W_s}{dx^2} \right] - D_{55} \frac{d^2\Psi}{dx^2} \right) \quad (11f)$$

where  $A$  stands for the cross-sectional areas of the microbeam. The symbol  $k_s$  appearing in shear force  $Q_1$  is a correction factor to consider the non-uniformity of shear strain over the microbeam cross-section [Ke et al. 2012; Reddy 2007]. Also, the stiffness constituents in these relations are defined as

$$\{A_{11}, B_{11}, D_{11}\} = \int_{-h/2}^{h/2} (\lambda(z) + 2\mu(z)) \{1, z, z^2\} dz, \quad \{A_{55}, B_{55}, D_{55}\} = \int_{-h/2}^{h/2} \mu(z) \{1, z, z^2\} dz. \quad (12)$$

The work  $\Pi_P$  done by the axial force  $\bar{N}_{0x}$  can be also written as

$$\Pi_P = \frac{1}{2} \int_0^L \bar{N}_{0x} \left( \frac{dW}{dx} \right)^2 dx. \quad (13)$$

Using (10) and (13) and implementing the principle of virtual work, the governing stability equations and corresponding boundary conditions of an FGM Timoshenko microbeam can be obtained as

$$\frac{dN_1}{dx} - \frac{d^2(P_1 + T_{111}^\tau)}{dx^2} = 0, \quad (14a)$$

$$\frac{d}{dx} \left\{ \left( N_1 - \bar{N}_{0x} - \frac{d(P_1 + T_{111}^\tau)}{dx} \right) \cdot \frac{dW}{dx} \right\} + \frac{dQ_1}{dx} + \frac{4}{3} \frac{dT_{333}^\tau}{dx^2} + \frac{1}{2} \frac{d^2Y_{12}}{dx^2} = 0, \quad (14b)$$

$$Q_1 - \frac{d(M_1 + P_3)}{dx} + \frac{d^2(M_1^p + M_{111}^\tau)}{dx^2} + \frac{8}{3} \frac{dT_{333}^\tau}{dx} = 0, \quad (14c)$$

$$\left( N_1 - \frac{d(P_1 + T_{111}^\tau)}{dx} \right) \Big|_{x=0,L} = 0 \quad \text{or} \quad \delta U|_{x=0,L} = 0, \quad (14d)$$

$$\left( (N_1 - \bar{N}_{0x}) \frac{dW}{dx} + Q_1 - \frac{d(P_1 + T_{111}^\tau)}{dx} \frac{d^2W}{dx^2} + \frac{4}{3} \frac{dT_{333}^\tau}{dx} + \frac{1}{2} \frac{dY_{12}}{dx} \right) \Big|_{x=0,L} = 0 \quad \text{or} \quad \delta W|_{x=0,L} = 0, \quad (14e)$$

$$\left( M_1 + P_3 - \frac{d(M_1^p + M_{111}^\tau)}{dx} - \frac{8}{3} T_{333}^\tau + \frac{Y_{12}}{2} \right) \Big|_{x=0,L} = 0 \quad \text{or} \quad \delta \Psi|_{x=0,L} = 0, \quad (14f)$$

$$(P_1 + T_{111}^\tau)|_{x=0,L} = 0 \quad \text{or} \quad \delta \left( \frac{dU}{dx} \right) \Big|_{x=0,L} = 0, \quad (14g)$$

$$\left( -(P_1 + T_{111}^\tau) \frac{dW}{dx} + \frac{4}{3} T_{333}^\tau + \frac{Y_{12}}{2} \right) \Big|_{x=0,L} = 0 \quad \text{or} \quad \delta \left( \frac{dW}{dx} \right) \Big|_{x=0,L} = 0, \quad (14h)$$

$$(M_1^p + M_{111}^\tau)|_{x=0,L} = 0 \quad \text{or} \quad \delta \left( \frac{d\Psi}{dx} \right) \Big|_{x=0,L} = 0. \quad (14i)$$

Accordingly, based on the MSGT, the stability equations and associated boundary conditions of a size-dependent FGM microbeam are derived. In effect, these relations can be reduced to the stability equations and associated boundary conditions of a FGM Timoshenko microbeam achieved by the MCST and CT, if two or three material length scale parameters set to be zero, respectively [Ke et al. 2012].

We introduce the parameters

$$\xi = \frac{x}{L}, \quad \eta = \frac{L}{h}, \quad (u, w, w_s) = \frac{(U, W, W_s)}{h}, \quad \psi = \Psi, \quad N_0 = \frac{\bar{N}_{0x}}{A_{110}}, \quad (\ell_0, \ell_1, \ell_2) = \frac{(l_0, l_1, l_2)}{h}, \quad (15a)$$

$$(a_{11}, a_{55}, b_{11}, b_{55}, d_{11}, d_{55}) = \left( \frac{A_{11}}{A_{110}}, \frac{A_{55}}{A_{110}}, \frac{B_{11}}{A_{110}h}, \frac{B_{55}}{A_{110}h}, \frac{D_{11}}{A_{110}h^2}, \frac{D_{55}}{A_{110}h^2} \right), \quad (15b)$$

$$c_1 = (2\ell_0^2 + \frac{4}{3}\ell_1^2), \quad c_2 = (\frac{8}{15}\ell_1^2 + \frac{1}{4}\ell_2^2), \quad c_3 = (\frac{16}{15}\ell_1^2 - \frac{1}{4}\ell_2^2), \quad c_4 = (2\ell_0^2 + \frac{32}{15}\ell_1^2 + \frac{1}{4}\ell_2^2) \quad (15c)$$



which  $A_{110}$  denotes the value of  $A_{11}$  of a homogeneous metal beam. The stability equations of the FGM microbeam can be rewritten as

$$a_{11} \frac{d^2 u}{d\xi^2} - \frac{a_{55} c_1}{\eta^2} \frac{d^4 u}{d\xi^4} - b_{11} \frac{d^2 \psi}{d\xi^2} + \frac{b_{55} c_1}{\eta^2} \frac{d^4 \psi}{d\xi^4} + \bar{Z}_1 = 0, \quad (16a)$$

$$k_s a_{55} \left( \frac{d^2 w}{d\xi^2} - \frac{d^2 w_s}{d\xi^2} - \eta \frac{d\psi}{d\xi} \right) - \frac{a_{55} c_2}{\eta^2} \left( \frac{d^4 w}{d\xi^4} - \frac{d^4 w_s}{d\xi^4} \right) + \frac{a_{55} c_3}{\eta} \frac{d^3 \psi}{d\xi^3} - N_0 \frac{d^2 w}{d\xi^2} + \bar{Z}_2 = 0, \quad (16b)$$

$$k_s a_{55} \eta \left( \frac{dw}{d\xi} - \frac{dw_s}{d\xi} - \eta \psi \right) - b_{11} \frac{d^2 u}{d\xi^2} + (d_{11} + c_4 a_{55}) \frac{d^2 \psi}{d\xi^2} + \frac{a_{55} c_3}{\eta} \left( \frac{\partial^3 w}{d\xi^3} - \frac{d^3 w_s}{d\xi^3} \right) + \frac{c_1}{\eta^2} \left[ b_{55} \frac{d^4 u}{d\xi^4} - d_{55} \frac{d^4 \psi}{d\xi^4} \right] + \bar{Z}_3 = 0, \quad (16c)$$

where

$$\bar{Z}_1 = \frac{a_{11}}{\eta} \frac{dw}{d\xi} \frac{d^2 w}{d\xi^2} - \frac{a_{55} c_1}{\eta^3} \left( \frac{dw}{d\xi} \frac{d^4 w}{d\xi^4} + 3 \frac{d^2 w}{d\xi^2} \frac{d^3 w}{d\xi^3} \right) - \frac{a_{11}}{\eta} \frac{dw_s}{d\xi} \frac{d^2 w_s}{d\xi^2} + \frac{a_{55} c_1}{\eta^3} \left( \frac{dw_s}{d\xi} \frac{d^4 w_s}{d\xi^4} + 3 \frac{d^2 w_s}{d\xi^2} \frac{d^3 w_s}{d\xi^3} \right), \quad (17a)$$

$$\begin{aligned} \bar{Z}_2 = & \frac{a_{11}}{\eta} \left[ \frac{du}{d\xi} \frac{d^2 w}{d\xi^2} + \frac{d^2 u}{d\xi^2} \frac{dw}{d\xi} + \frac{3}{2\eta} \left( \frac{dw}{d\xi} \right)^2 \frac{d^2 w}{d\xi^2} \right] + \frac{b_{55} c_1}{\eta^3} \left[ \frac{dw}{d\xi} \frac{d^4 \psi}{d\xi^4} + \frac{d^2 w}{d\xi^2} \frac{d^3 \psi}{d\xi^3} \right] \\ & - \frac{a_{55} c_1}{\eta^3} \left[ \frac{d^4 u}{d\xi^4} \frac{dw}{d\xi} + \frac{d^3 u}{d\xi^3} \frac{d^2 w}{d\xi^2} + \frac{1}{\eta} \left( \frac{d^2 w}{d\xi^2} \right)^3 + \frac{4}{\eta} \frac{dw}{d\xi} \frac{d^2 w}{d\xi^2} \frac{d^3 w}{d\xi^3} + \frac{1}{\eta} \left( \frac{dw}{d\xi} \right)^2 \frac{d^4 w}{d\xi^4} \right] \\ & - \frac{b_{11}}{\eta} \left( \frac{d^2 w}{d\xi^2} \frac{d\psi}{d\xi} + \frac{dw}{d\xi} \frac{d^2 \psi}{d\xi^2} \right) - \frac{a_{11}}{2\eta^2} \left( \frac{dw_s}{d\xi} \right)^2 \frac{\partial^2 w}{d\xi^2} - \frac{a_{11}}{\eta^2} \frac{dw}{d\xi} \frac{dw_s}{d\xi} \frac{d^2 w_s}{d\xi^2} \\ & + \frac{a_{55} c_1}{\eta^4} \left( \frac{d^2 w}{d\xi^2} \frac{dw_s}{d\xi} \frac{d^2 w_s}{d\xi^2} + 3 \frac{d^2 w_s}{d\xi^2} \frac{dw}{d\xi} \frac{d^3 w_s}{d\xi^3} + \left( \frac{d^2 w_s}{d\xi^2} \right)^2 \frac{d^2 w}{d\xi^2} + \frac{dw}{d\xi} \frac{dw_s}{d\xi} \frac{d^4 w_s}{d\xi^4} \right), \quad (17b) \end{aligned}$$

$$\begin{aligned} \bar{Z}_3 = & \frac{b_{55} c_1}{\eta^3} \left[ 3 \frac{d^2 w}{d\xi^2} \frac{d^3 w}{d\xi^3} + \frac{dw}{d\xi} \frac{\partial^4 w}{d\xi^4} \right] - \frac{b_{11}}{\eta} \frac{dw}{d\xi} \frac{d^2 w}{d\xi^2} + \frac{b_{11}}{\eta} \frac{dw_s}{d\xi} \frac{d^2 w_s}{d\xi^2} \\ & - \frac{b_{55} c_1}{\eta^3} \left( \frac{dw_s}{d\xi} \frac{d^4 w_s}{d\xi^4} + 3 \frac{d^2 w_s}{d\xi^2} \frac{d^3 w_s}{d\xi^3} \right). \quad (17c) \end{aligned}$$

Also, depending on the type of end conditions, the boundary conditions of the FGM microbeam can be as follows:

For clamped (C) end condition

$$u = w = \psi = \frac{du}{d\xi} = \frac{dw}{d\xi} = \frac{d\psi}{d\xi} = 0. \quad (18)$$

For simply-supported (SS) end condition

$$\begin{aligned} u = w &= a_{55} \left( \frac{d^2 u}{d\xi^2} + \frac{1}{\eta} \frac{dw}{d\xi} \frac{d^2 w}{d\xi^2} \right) - b_{55} \frac{d^2 \psi}{d\xi^2} \\ &= b_{55} \left( \frac{d^2 u}{d\xi^2} + \frac{1}{\eta} \frac{dw}{d\xi} \frac{d^2 w}{d\xi^2} - \frac{1}{\eta} \frac{dw_s}{d\xi} \frac{d^2 w_s}{d\xi^2} \right) - d_{55} \frac{d^2 \psi}{d\xi^2} = 0, \end{aligned} \quad (19a)$$

$$\begin{aligned} -c_1 \left( \frac{a_{55} d^2 w}{\eta^3 d\xi^2} \left( \frac{dw}{d\xi} \right)^2 - \frac{a_{55} d^2 w_s}{\eta^3 d\xi^2} \frac{dw_s}{d\xi} \frac{dw}{d\xi} + \frac{a_{55} dw}{\eta^2 d\xi} \frac{d^2 u}{d\xi^2} - \frac{b_{55} dw}{\eta^2 d\xi} \frac{d^2 \psi}{d\xi^2} \right) \\ - \frac{a_{55} c_2}{\eta^3} \frac{d^2 w}{d\xi^2} + a_{55} c_3 \frac{d\psi}{d\xi} = 0, \end{aligned} \quad (19b)$$

$$\begin{aligned} b_{11} \left( \frac{du}{d\xi} + \frac{1}{2\eta} \left( \frac{dw}{d\xi} \right)^2 - \frac{1}{2\eta} \left( \frac{dw_s}{d\xi} \right)^2 \right) - d_{11} \frac{d\psi}{d\xi} + \frac{d_{55} c_1}{\eta^2} \frac{d^3 \psi}{d\xi^3} + \frac{a_{55} c_3}{\eta} \frac{d^2 w}{d\xi^2} - a_{55} c_4 \frac{d\psi}{d\xi} \\ + c_1 \left( -\frac{b_{55} d^3 u}{\eta^2 d\xi^3} - \frac{b_{55} dw}{\eta^3 d\xi} \frac{d^3 w}{d\xi^3} + \frac{b_{55} dw_s}{\eta^3 d\xi} \frac{d^3 w_s}{d\xi^3} - \frac{b_{55}}{\eta^3} \left( \frac{d^2 w}{d\xi^2} \right)^2 + \frac{b_{55}}{\eta^3} \left( \frac{d^2 w_s}{d\xi^2} \right)^2 \right) = 0. \end{aligned} \quad (19c)$$

## 5. Numerical solution

Various numerical techniques are available to solve the present stability equations and associated boundary conditions. Herein, the GDQ method [Shu 2000] is utilized to discretize the stability equations and boundary conditions. This technique has exhibited a great potential in solving large partial differential equations [Ansari et al. 2012a; 2012b]. In this work, for sake of brevity, we avoid presenting the discretized counterparts of stability equations and corresponding boundary conditions. Substituting the equations of the boundary conditions into the equations of the system in the boundaries leads to a set of nonlinear equations of the domain coupled with the boundary as

$$\mathbf{F} : \mathbb{R}^{3n+1} \rightarrow \mathbb{R}^{3n}, \quad \mathbf{F}(\mathbf{v}, N_0) = 0, \quad \mathbf{v} = \{\mathbf{u}^T, \mathbf{w}^T, \boldsymbol{\psi}^T\}^T \quad (20)$$

in which  $n$  is the number of grid points in the GDQ discretization;  $\mathbf{v}$  and  $N_0$  denote the field variable vector dictating the buckling deformation and the buckling load, respectively. This nonlinear load-deflection equation is rather large and can be hardly treated through a linearization scheme. Therefore, another solution strategy is adopted herein which does not need any linearization. Since the buckling load  $N_0$  itself is unknown, the number of unknown variables is one more than the number of the equations appearing in (20). To rectify this problem, a normalizing equation is added to (20) to convert the present eigenvalue problem to a set of nonlinear equations of the form

$$\begin{aligned} \mathbf{F}(\mathbf{v}, N_0) &= 0, \\ \mathbf{v}^T \mathbf{v} - c &= 0. \end{aligned} \quad (21)$$

Now, the preceding nonlinear equations can be solved by implementing the Newton method, provided that the initial values are selected appropriately. To this end, the equations are solved first by dropping the nonlinear terms. Then, the linear response is imparted to the nonlinear equations in Newton's method as initial values so as to obtain eigenpairs of the nonlinear model.

## 6. Results and discussion

In this section, the buckling and postbuckling analyses of FGM Timoshenko microbeams undergoing an axial compressive load with different boundary conditions are represented. FGM microbeams made of a mixture of aluminum (Al) and ceramic (SiC) with material properties of  $E_m = 70$  GPa,  $\nu_m = 0.3$ ,  $\rho_m = 2702$  kg/m<sup>3</sup> for Al, and  $E_c = 427$  GPa,  $\nu_c = 0.17$ ,  $\rho_c = 3100$  kg/m<sup>3</sup> for SiC are considered. The materials at bottom surface and top surface of the microbeam are considered to be metal-rich and ceramic-rich, respectively.

In order to evaluate the length scale parameters, it is necessary to have experimental data of a homogeneous epoxy or FGM microbeam. Lam et al. [2003] experimentally approximated the length scale parameter of an isotropic homogeneous microbeam as  $l = 17.6$   $\mu\text{m}$ . To our best knowledge, there is no experimental report concerned with FGM microbeams in the literature. To have a quantitative analysis on the size effect of the FGM microbeams, the values of each length scale parameter are set to be  $l = 15$   $\mu\text{m}$ .

In the following subsections, based upon the above-mentioned assumptions, firstly, the size-dependent buckling behavior of FGM microbeams is described; then the postbuckling analysis of FGM microbeams is performed. Numerical analyses are accomplished for FGM microbeams with three commonly-used end conditions including SS-SS, C-SS and C-C boundary conditions.

**Buckling analysis.** Table 1 reports the first five non-dimensional buckling loads predicted by the MSGT for C-C, C-SS, and SS-SS microbeams with different material gradient indexes. It is seen that non-dimensional buckling loads decreases with the rise of material gradient index. Hence, the stability of

Boundary conditions	Mode	Ceramic	$k = 0.1$	$k = 1$	$k = 10$	Metal
C-C	1	0.1119	0.107	0.0864	0.067	0.0622
	2	0.1756	0.1679	0.1351	0.104	0.0967
	3	0.2704	0.2585	0.2075	0.1588	0.1477
	4	0.3321	0.3174	0.2544	0.194	0.1805
	5	0.4190	0.4004	0.3206	0.2439	0.2269
C-SS	1	0.0651	0.0623	0.0504	0.0393	0.0364
	2	0.1477	0.1412	0.1139	0.0879	0.0817
	3	0.2292	0.2191	0.1761	0.1351	0.1255
	4	0.3035	0.2901	0.2327	0.1777	0.1653
	5	0.3786	0.3618	0.2898	0.2207	0.2053
SS-SS	1	0.035	0.0335	0.0273	0.0212	0.0197
	2	0.1119	0.107	0.0864	0.067	0.0622
	3	0.1939	0.1854	0.1492	0.1148	0.1067
	4	0.2704	0.2585	0.2075	0.1588	0.1477
	5	0.3441	0.3289	0.2636	0.201	0.1869

**Table 1.** First five non-dimensional buckling loads for different gradient material indexes ( $k$ ) of FGM microbeams with C-C, C-SS, and SS-SS end conditions ( $h/l = 2$ ,  $L/h = 12$ ).

Boundary conditions	Mode	$h/l = 1$	$h/l = 2$	$h/l = 3$	$h/l = 6$	$h/l = 8$	$h/l = 16$	CT
C-C	1	0.1989	0.0864	0.0525	0.0276	0.0235	0.0194	0.0178
	2	0.2891	0.1351	0.0882	0.0497	0.0429	0.0359	0.0331
	3	0.4468	0.2075	0.141	0.0837	0.0731	0.0618	0.0573
	4	0.583	0.2544	0.1744	0.1075	0.0947	0.081	0.0755
	5	0.7831	0.3206	0.2181	0.1363	0.1207	0.1038	0.097
C-SS	1	0.1284	0.0504	0.0294	0.0149	0.0126	0.0103	0.0094
	2	0.2479	0.1139	0.0721	0.0392	0.0337	0.028	0.0258
	3	0.3727	0.1761	0.1178	0.0682	0.0592	0.0497	0.046
	4	0.5158	0.2327	0.1593	0.0966	0.0848	0.0721	0.0671
	5	0.6836	0.2898	0.1985	0.1234	0.109	0.0934	0.0872
SS-SS	1	0.0792	0.0273	0.0153	0.0075	0.0063	0.0052	0.0047
	2	0.1989	0.0864	0.0526	0.0276	0.0235	0.0194	0.0178
	3	0.3159	0.1492	0.0975	0.0548	0.0473	0.0395	0.0364
	4	0.4468	0.2075	0.141	0.0837	0.0731	0.0618	0.0573
	5	0.6013	0.2636	0.181	0.1113	0.098	0.0837	0.078

**Table 2.** First five non-dimensional buckling loads for different non-dimensional length scale parameters ( $h/l$ ) of FGM microbeams with C-C, C-SS, and S-SS end conditions ( $k = 1$ ,  $L/h = 12$ ).

fully ceramic microbeams is larger than that of microbeams with lower material gradient indexes. Also, it is seen that the values of the critical buckling load in microbeams with C-C end conditions are more than those for SS-SS and C-SS counterparts which signifies that C-C microbeams are more stable than other counterparts.

Table 2 is represented to highlight the effect of the non-dimensional length scale parameter  $h/l$  on the first five non-dimensional buckling loads of FGM microbeams with three different boundary conditions. It is seen that the value of non-dimensional buckling load reduces with the increase of the non-dimensional length scale parameter, in a way that at lower non-dimensional length scale parameters, this decrement is very considerable, while when the values increases, there is no prominent changes. Accordingly, the CT underestimates the non-dimensional critical buckling loads, especially at lower non-dimensional length scale parameters.

Table 3 reveals the first five non-dimensional buckling loads corresponding to different slenderness ratios  $L/h$  of FGM microbeams with three boundary conditions. It is shown that an increase in the slenderness ratio leads to lower values of non-dimensional buckling loads in a way that this reduction is more evident in higher buckling modes. Accordingly, the possibility of buckling increases at higher slenderness ratios and microbeams with lower slenderness ratios can resist more axial compressive loads.

Figure 2 compares the non-dimensional critical buckling loads predicted by the MSGT, MCST and CT versus the non-dimensional length scale parameter  $h/l$ . The figure is plotted for FGM microbeams with SS-SS, C-SS and C-C boundary conditions. With an increase in non-dimensional length scale parameter, the non-dimensional critical buckling load shows a downward trend. Also, it is seen that non-dimensional

Boundary conditions	Mode	$L/h = 8$	$L/h = 10$	$L/h = 12$	$L/h = 16$	$L/h = 20$
C-C	1	0.0992	0.0709	0.0525	0.0316	0.0209
	2	0.1476	0.1128	0.0882	0.057	0.0392
	3	0.2195	0.1739	0.141	0.0966	0.0691
	4	0.2629	0.2108	0.1744	0.1249	0.0928
	5	0.3262	0.2613	0.2181	0.1605	0.1225
C-SS	1	0.0597	0.0408	0.0294	0.0171	0.0111
	2	0.1271	0.0944	0.0721	0.045	0.0303
	3	0.1892	0.1477	0.1178	0.0785	0.055
	4	0.2428	0.1941	0.1593	0.1119	0.0816
	5	0.297	0.2385	0.1985	0.1443	0.1087
SS-SS	1	0.0331	0.0217	0.0153	0.0086	0.0055
	2	0.0992	0.0709	0.0526	0.0317	0.0209
	3	0.1633	0.1248	0.0975	0.0629	0.0432
	4	0.2195	0.1739	0.141	0.0966	0.0691
	5	0.2725	0.2187	0.181	0.1295	0.0961

**Table 3.** First five non-dimensional buckling loads for different slenderness ratios ( $L/h$ ) of FGM microbeams with C-C, C-SS, and SS-SS end conditions ( $h/l = 3$ ,  $k = 1$ ).

critical buckling loads predicted by the CT and MCST are lower than those of the MSGT; in other words, the CT and MCST underestimate the non-dimensional critical buckling loads. Moreover, the difference between the values predicted by classical and non-classical theories get really pronounced at small values of non-dimensional length scale parameter which confirms the importance of using the MSGT theory at lower non-dimensional length scale parameters. However, it is seen that as the values of the non-dimensional length scale parameter grow, the difference between the values predicted by classical and non-classical theories fades. Furthermore, non-dimensional critical buckling loads of the microbeam with C-C end conditions are significantly more than those for other counterparts.

**Postbuckling analysis.** Figures 3 to 6 are represented to provide an accurate insight into the postbuckling behavior of FGM microbeams with C-C, C-SS and SS-SS boundary conditions. All figures illustrate the non-dimensional deflection of FGM microbeams versus the non-dimensional applied axial load for FGM microbeams with C-C, C-SS and SS-SS boundary conditions.

Figure 3 is depicted to highlight the influence of the material gradient index  $k$  on the postbuckling behavior of FGM microbeams with C-C, C-SS and SS-SS boundary conditions. As can be seen, the non-dimensional deflection soars sharply with increasing the applied axial load. An increase in the material gradient index shifts the graphs to the left-hand side in all types of boundary conditions and induces more large postbuckled deflections which indicates that the stability decreases. Moreover, when the type of boundary conditions comes to SS-SS microbeams, the graphs get closer which signify that the effect of material gradient index is more prominent in microbeams with C-C end conditions. Besides, the slope of graphs in SS-SS microbeams is much higher than that of microbeams with C-SS and C-C end conditions.

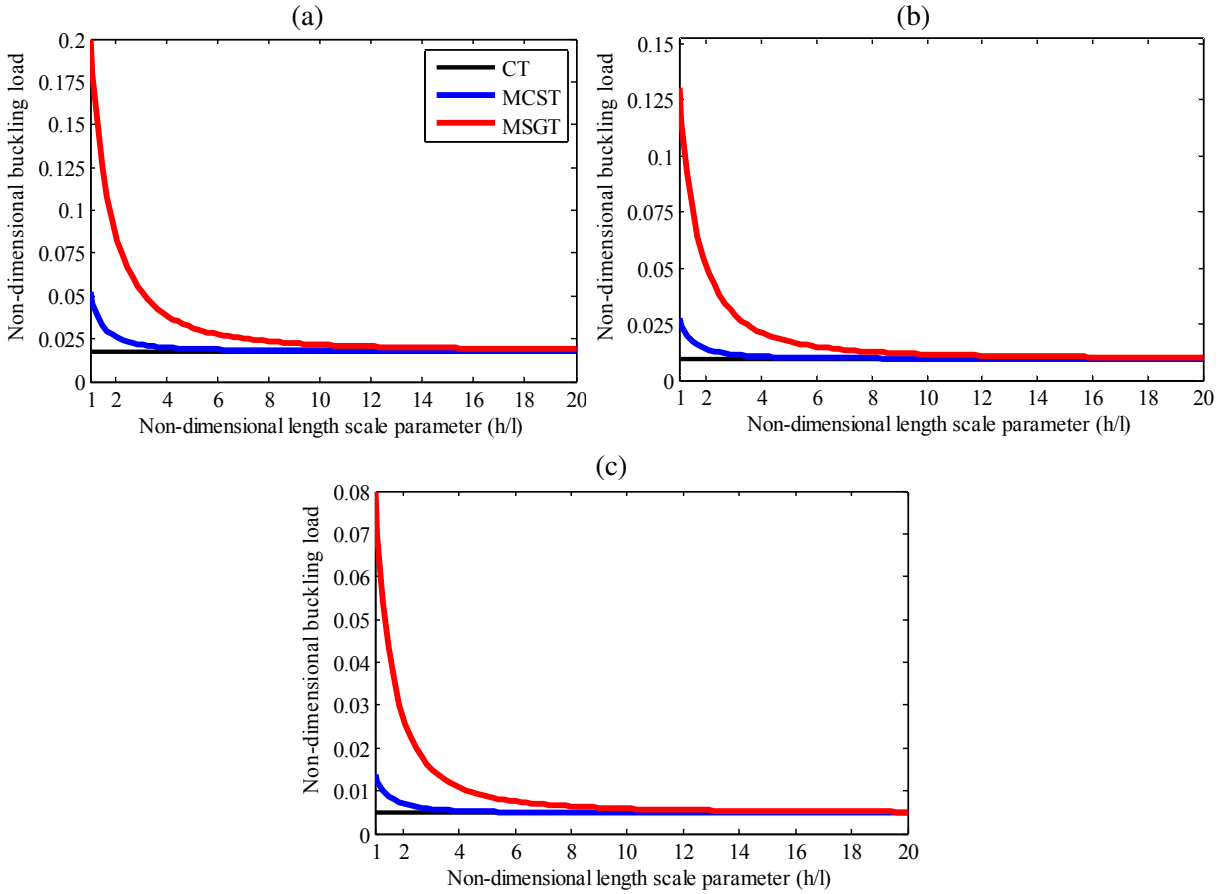


**Figure 2.** Non-dimensional critical buckling loads predicted by the MSGT, MCST and CT versus non-dimensional length scale parameter ( $h/l$ ) of FGM microbeams with C-C, C-SS, and SS-SS end conditions ( $k = 1$ ,  $L/h = 12$ ) (a) C-C microbeam, (b) C-SS microbeam, and (c) SS-SS microbeam.

Effect of the non-dimensional length scale parameter  $h/l$  on the non-dimensional deflection of FGM microbeams with three types of boundary conditions is investigated in Figure 4. It is observed that a decrease in the value of non-dimensional length scale parameter shifts the graphs to the right-hand side. In other words, CT underestimates the non-dimensional critical axial load. Also, by comparing these three plots, it is seen that the difference between graphs is really significant in C-C microbeams which signal the necessity of using the MSGT theory in studying postbuckling behavior of microbeams with C-C end conditions compared to other end conditions.

Figure 5 reveals the influence of slenderness ratio  $L/h$  on the postbuckling behavior of FGM microbeams with C-C, C-SS and SS-SS boundary conditions. With increasing the slenderness ratio of FGM microbeams, the graphs move to the left-hand side which indicates that the stability declines. Also, it is observed that at higher slenderness ratios, a small rise in the applied axial load leads to a sharp increase in the non-dimensional deflection, while at lower slenderness ratios, the non-dimensional

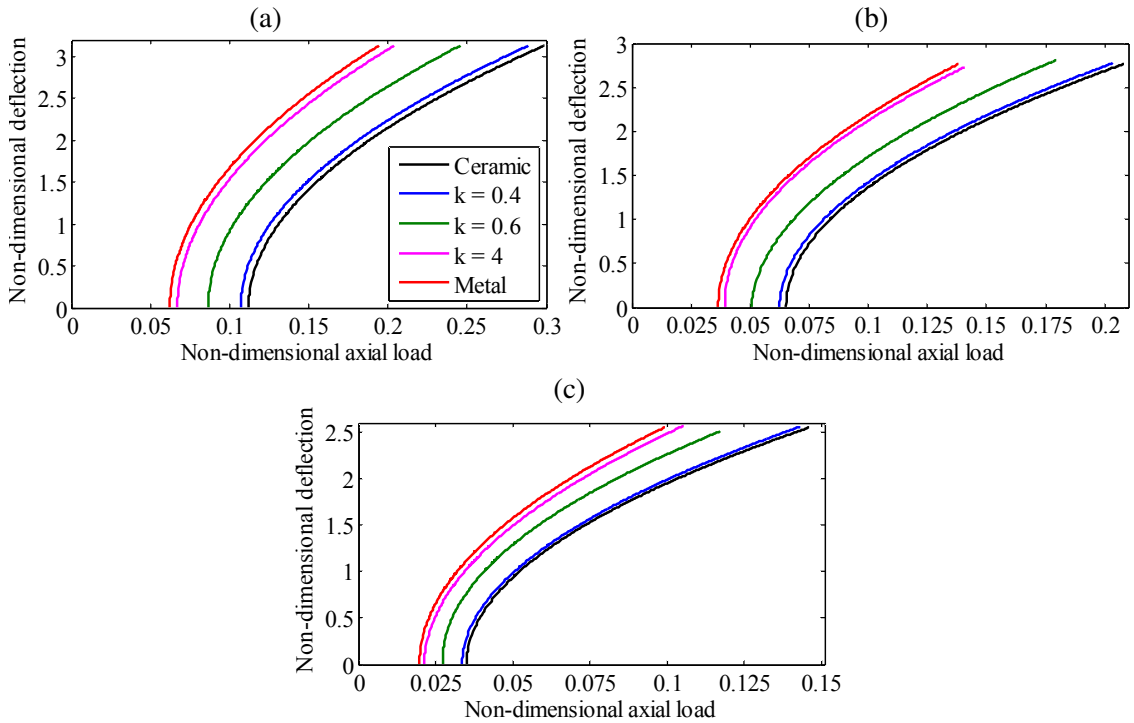


**Figure 3.** Non-dimensional deflection versus the non-dimensional axial load for different material gradient indexes ( $k$ ) of FGM microbeams with C-C, C-SS, and SS-SS end conditions ( $h/l = 2$ ,  $L/h = 12$ ) (a) C-C microbeam, (b) C-SS microbeam, and (c) SS-SS microbeam.

deflection increases gradually. So, microbeams with lower slenderness ratios are much stronger than those with larger ones. Furthermore, the graphs are comparatively closer in microbeams with SS-SS end conditions. Hence, microbeams with C-C boundary conditions are more strongly affected by slenderness ratio compared to SS-SS and C-SS counterparts.

Figure 6 compares the non-dimensional deflection of FGM microbeams predicted by the MSGT and CT versus non-dimensional axial load for the first three modes. As it was mentioned earlier, here it is seen that the CT underestimates the non-dimensional critical axial load, especially at higher modes which confirms the necessity of using the MSGT theory at higher postbuckling modes.

Figure 7 illustrates the effect of the imperfection on the non-dimensional deflection of the microbeams versus non-dimensional applied load for first three postbuckling modes of FGM microbeams with different end conditions. Imperfection is treated here by the pre-deformation  $W_s$  of the microbeam in its unstressed state.  $\gamma$  is a small dimensionless parameter proportional to the maximum pre-deformation  $W_s^{\max}$  at a certain characteristic length  $L$ , i.e.,  $W_s^{\max} = \gamma L$ . This implies that the magnitude of imperfection (the proportionality factor  $\gamma$ ) is reasonably scaled with the structure size. To achieve higher postbuckling deformation mode, the linear buckling deformation with the maximum amplitude of  $W_s^{\max}$  corresponding to that mode is chosen as the pre-deformation. As it is demonstrated in this figure, for ideal loading and geometry  $\gamma = 0$ , there is no deflection at prebuckling region, while as imperfection

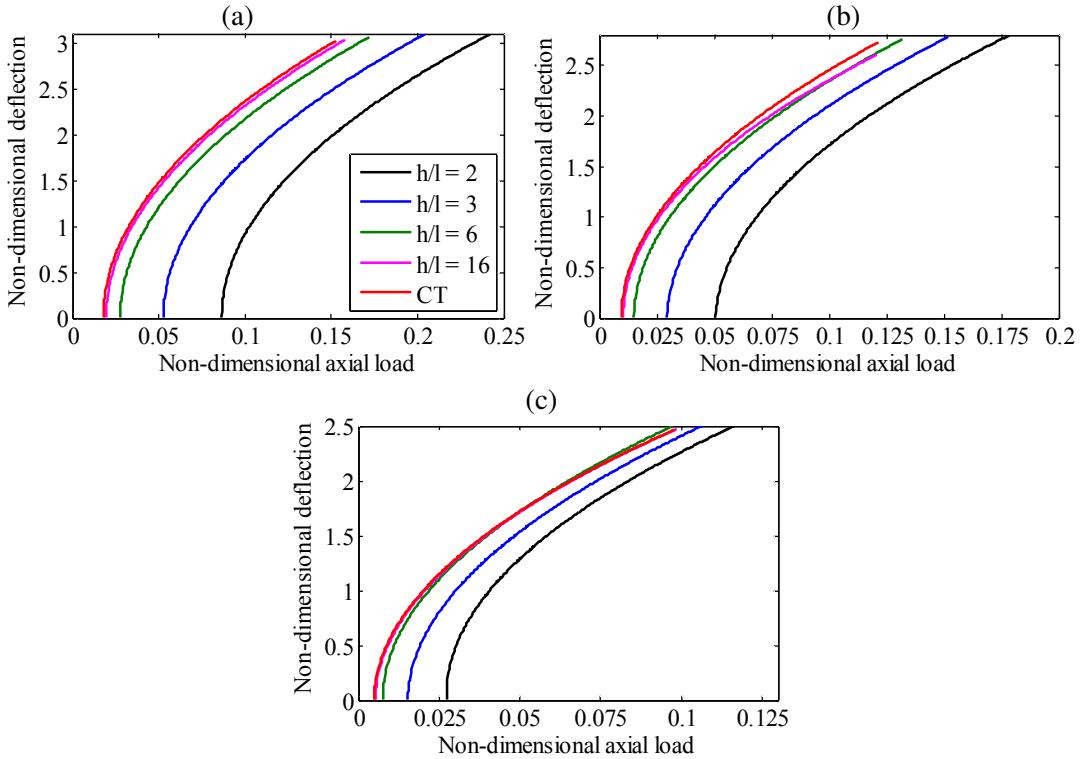


**Figure 4.** Non-dimensional deflection versus the non-dimensional axial load for different non-dimensional length scale parameter ( $h/l$ ) of FGM microbeams with C-C, C-SS, and SS-SS end conditions ( $k = 1$ ,  $L/h = 12$ ) (a) C-C microbeam, (b) C-SS microbeam, and (c) SS-SS microbeam.

grows, the deviation between the ideal microbeam and imperfect counterparts continue to increase. This deviation even grows at higher modes and considerably affects the buckling deflection, especially at critical axial loads. In addition, it is evident that the difference between ideal and non-ideal beam is more prominent at microbeams with C-C end supports which signify that C-C microbeams are more sensitive to imperfections compared to other counterparts.

## 7. Conclusion

In this work, the buckling and postbuckling of FGM microbeams were studied based on the MSGT. By employing the power law function, the volume fraction of the ceramic and metal phases of the FGM microbeams was described. According to the nonlinear Timoshenko beam theory and Hamilton's principle, the higher-order governing differential equations and corresponding boundary conditions were derived and solved through the GDQ method in conjunction with a direct approach without linearization. The effect of imperfection on the non-dimensional deflection of microbeams was considered. The effects of the length scale parameter, slenderness ratio, material gradient index and boundary conditions on the critical buckling load and postbuckling deflection of FGM Timoshenko microbeams were carefully



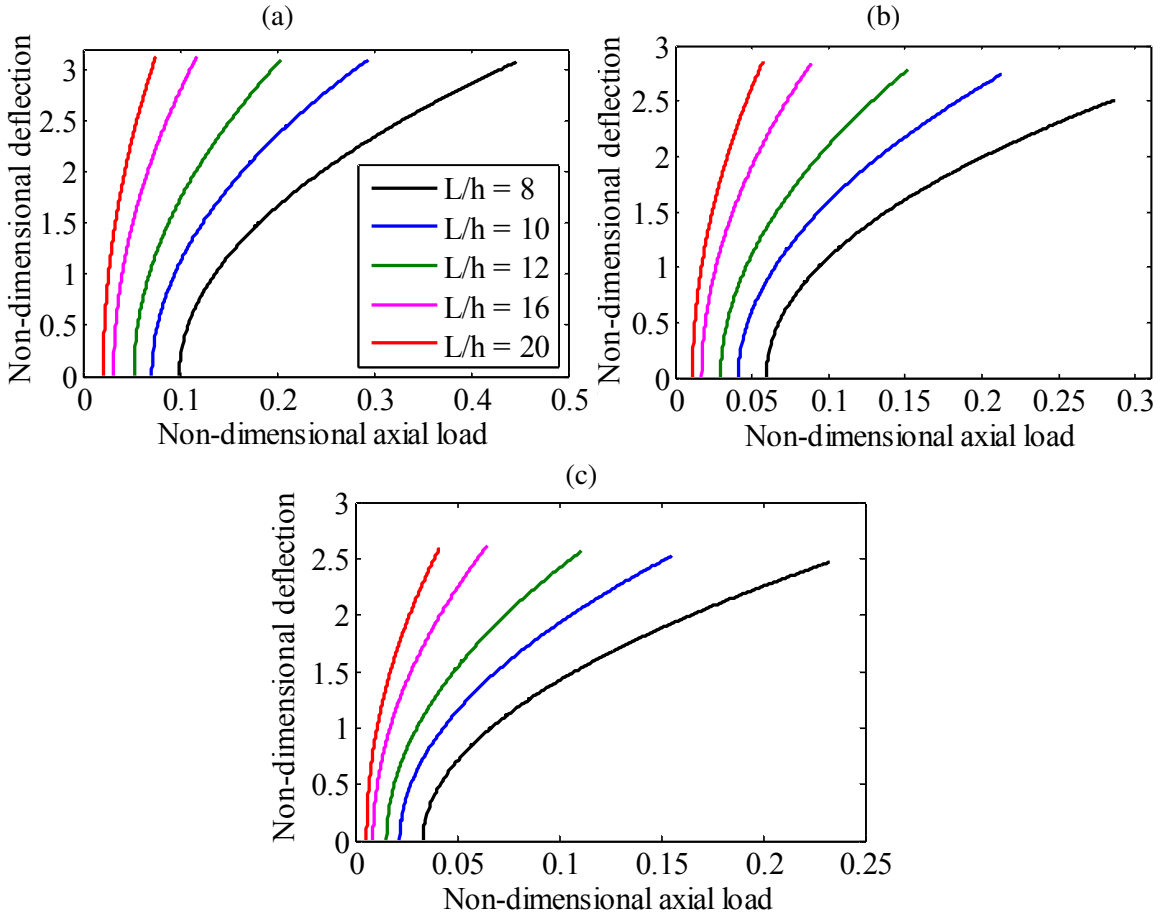


**Figure 5.** Non-dimensional deflection versus the non-dimensional axial load for different slenderness ratios  $L/h$  of FGM microbeams with C-C, C-SS, and SS-SS end conditions ( $k = 1$ ,  $h/l = 3$ ) (a) C-C microbeam, (b) C-SS microbeam, and (c) SS-SS microbeam.

investigated. It was observed that with an increase in material gradient index, the non-dimensional critical buckling loads and postbuckled deflections decreases and increases, respectively. With raising the non-dimensional length scale parameter, the value of non-dimensional critical buckling load reduces; hence, the CT and MCST underestimate the non-dimensional critical buckling loads, especially for C-C microbeams at lower non-dimensional length scale parameters. The larger slenderness ratio, lower values of non-dimensional critical buckling loads; so, microbeams with lower slenderness ratios can resist more axial compressive loads. The effects of material gradient index and slenderness ratio are more prominent in microbeams with C-C end conditions compared to SS-SS and C-SS counterparts. Also, it was seen that the values of the critical buckling load in microbeams with C-C end conditions are more than those for SS-SS and C-SS counterparts. In addition, we found that the imperfection considerably affects the buckling deflection of FGM microbeams, especially at critical axial loads.

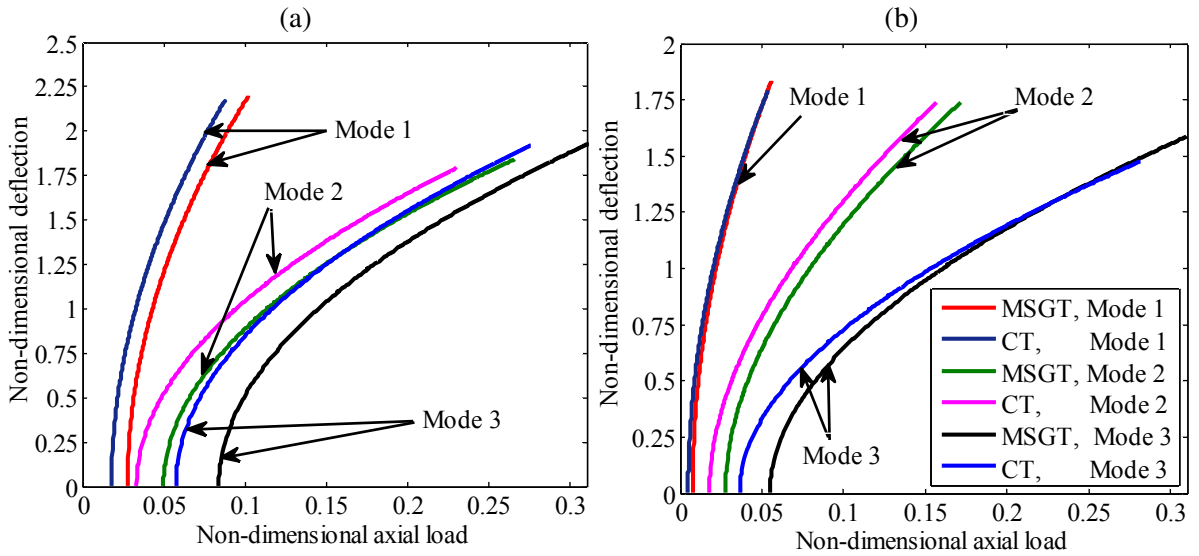


**Figure 6.** Non-dimensional deflection of FGM microbeams predicted by the MSGT and CT versus non-dimensional axial load for the first three postbuckling modes of FGM microbeams with C-C and SS-SS end conditions ( $k = 1$ ,  $h/l = 6$ ,  $L/h = 12$ ) (a) C-C microbeam, and (b) SS-SS microbeam.

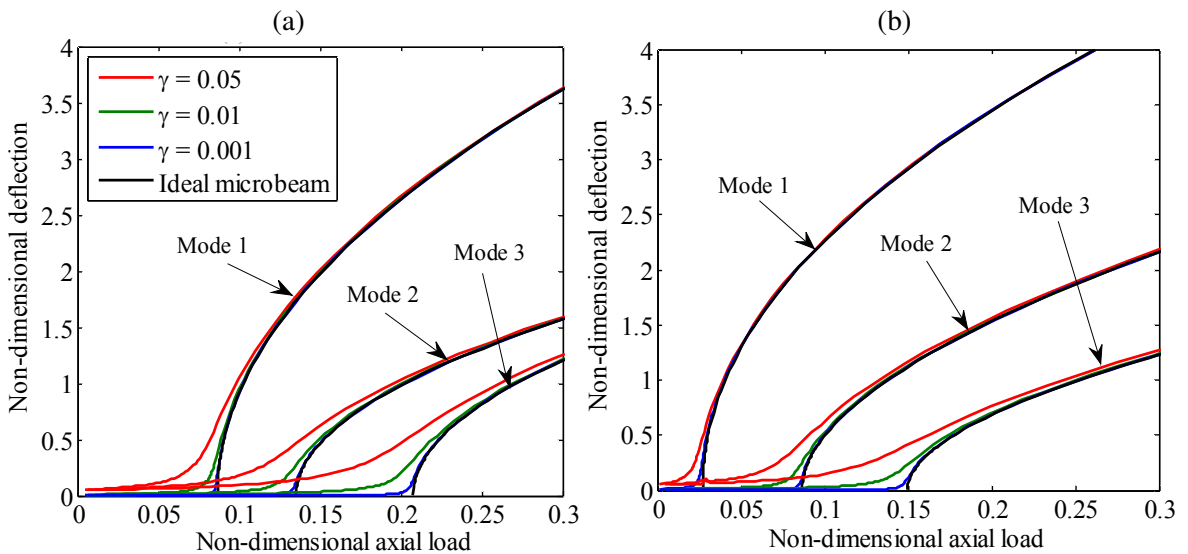


**Figure 7.** Effect of the imperfection on the non-dimensional deflection versus non-dimensional axial load for first three postbuckling modes of FGM microbeams with C-C and SS-SS end conditions ( $L/h = 12$ ,  $k = 1$ ,  $h/l = 2$ ) (a) C-C microbeam, and (b) SS-SS microbeam.

## References

- [Aifantis 1999] E. C. Aifantis, “Strain gradient interpretation of size effects”, *Int. J. Fract.* **95**:1–4 (1999), 299–314.
- [Ansari et al. 2011] R. Ansari, R. Gholami, and S. Sahmani, “Free vibration analysis of size-dependent functionally graded microbeams based on the strain gradient Timoshenko beam theory”, *Compos. Struct.* **94** (2011), 221–228.
- [Ansari et al. 2012a] R. Ansari, R. Gholami, and M. A. Darabi, “A nonlinear Timoshenko beam formulation based on a strain gradient theory”, *J. Mech. Mater. Struct.* **7**:2 (2012), 195–212.
- [Ansari et al. 2012b] R. Ansari, R. Gholami, and S. Sahmani, “Study of small scale effects on the nonlinear vibration response of functionally graded Timoshenko microbeams based on the strain gradient theory”, *J. Comput. Nonlinear Dyn. (ASME)* **7**:3 (2012), Art. ID #031009.
- [Asghari et al. 2010] M. Asghari, M. T. Ahmadian, M. H. Kahrobaian, and M. Rahaeifard, “On the size-dependent behavior of functionally graded micro-beams”, *Mater. Des.* **31** (2010), 2324–2329.
- [Asghari et al. 2011] M. Asghari, M. Rahaeifard, M. H. Kahrobaian, and M. T. Ahmadian, “The modified couple stress functionally graded Timoshenko beam formulation”, *Mater. Des.* **32** (2011), 1435–1443.
- [Eringen 1972] A. C. Eringen, “Nonlocal polar elastic continua”, *Int. J. Eng. Sci.* **10**:1 (1972), 1–16.
- [Fares et al. 2009] M. E. Fares, M. K. Elmarghany, and D. Atta, “An efficient and simple refined theory for bending and vibration of functionally graded plates”, *Compos. Struct.* **91** (2009), 296–305.
- [Fleck and Hutchinson 1993] N. A. Fleck and J. W. Hutchinson, “A phenomenological theory for strain gradient effects in plasticity”, *J. Mech. Phys. Solids* **41**:12 (1993), 1825–1857.
- [Fu et al. 2004] Y. Q. Fu, H. J. Du, W. M. Huang, S. Zhang, and M. Hu, “TiNi-based thin films in MEMS applications: a review”, *Sens. Actuators A Phys.* **112** (2004), 395–408.
- [Gurtin et al. 1998] M. E. Gurtin, J. Weissmuller, and F. Larche, “A general theory of curved deformable interfaces in solids at equilibrium”, *Philos. Mag. A* **78**:5 (1998), 1093–1109.
- [Hasanyan et al. 2008] D. J. Hasanyan, R. C. Batra, and R. C. Harutyunyan, “Pull-in instabilities in functionally graded microthermoelectromechanical systems”, *J. Therm. Stresses* **31** (2008), 1006–1021.
- [Kahrobaian et al. 2011] M. H. Kahrobaian, M. Asghari, M. Rahaeifard, and M. T. Ahmadian, “A nonlinear strain gradient beam formulation”, *Int. J. Eng. Sci.* **49**:11 (2011), 1256–1267.
- [Ke and Wang 2011] L.-L. Ke and Y.-S. Wang, “Size effect on dynamic stability of functionally graded microbeams based on a modified couple stress theory”, *Compos. Struct.* **93**:2 (2011), 342–350.
- [Ke et al. 2010] L.-L. Ke, J. Yang, and S. Kitipornchai, “An analytical study on the nonlinear vibration of functionally graded beams”, *Meccanica (Milano)* **45**:6 (2010), 743–752.
- [Ke et al. 2012] L.-L. Ke, Y.-S. Wang, J. Yang, and S. Kitipornchai, “Nonlinear free vibration of size-dependent functionally graded microbeams”, *Int. J. Eng. Sci.* **50**:1 (2012), 256–267.
- [Koiter 1964] W. T. Koiter, “Couple-stresses in the theory of elasticity: I and II”, *P. K. Ned. Akad. Wetensc. B* **67** (1964), 17–29 and 30–44.
- [Kong et al. 2009] S. Kong, S. Zhou, Z. Nie, and K. Wang, “Static and dynamic analysis of micro beams based on strain gradient elasticity theory”, *Int. J. Eng. Sci.* **47**:4 (2009), 487–498.
- [Lam et al. 2003] D. C. C. Lam, F. Yang, A. C. M. Chong, J. Wang, and P. Tong, “Experiments and theory in strain gradient elasticity”, *J. Mech. Phys. Solids* **51**:8 (2003), 1477–1508.
- [Ma et al. 2008] H. M. Ma, X.-L. Gao, and J. N. Reddy, “A microstructure-dependent Timoshenko beam model based on a modified couple stress theory”, *J. Mech. Phys. Solids* **56**:12 (2008), 3379–3391.
- [Ma et al. 2010] H. M. Ma, X.-L. Gao, and J. N. Reddy, “A nonclassical Reddy–Levinson beam model based on the a modified couple stress theory”, *J. Multiscale Comput. Eng.* **8** (2010), 167–180.
- [Ma et al. 2011] H. M. Ma, X.-L. Gao, and J. N. Reddy, “A non-classical Mindlin plate model based on a modified couple stress theory”, *Acta Mech.* **220**:1–4 (2011), 217–235.
- [Mindlin 1964] R. D. Mindlin, “Micro-structure in linear elasticity”, *Arch. Ration. Mech. Anal.* **16** (1964), 51–78.

- [Mindlin 1965] R. D. Mindlin, “Second gradient of strain and surface tension in linear elasticity”, *Int. J. Solids Struct.* **1**:4 (1965), 417–438.
- [Mindlin and Eshel 1968] R. D. Mindlin and N. N. Eshel, “On first strain-gradient theories in linear elasticity”, *Int. J. Solids Struct.* **4** (1968), 109–124.
- [Mindlin and Tiersten 1962] R. D. Mindlin and H. F. Tiersten, “Effects of couple-stresses in linear elasticity”, *Arch. Ration. Mech. Anal.* **11** (1962), 415–448.
- [Mirzavand and Eslami 2011] B. Mirzavand and M. R. Eslami, “A closed-form solution for thermal buckling of piezoelectric FGM rectangular plates with temperature-dependent properties”, *Acta Mech.* **218** (2011), 87–101.
- [Mohammadi-Alasti et al. 2011] B. Mohammadi-Alasti, G. Rezazadeh, A. M. Borgheei, S. Minaei, and R. Habibifar, “On the mechanical behavior of a functionally graded micro-beam subjected to a thermal moment and nonlinear electrostatic pressure”, *Compos. Struct.* **93** (2011), 1516–1525.
- [Park and Gao 2006] S. K. Park and X.-L. Gao, “Bernoulli–Euler beam model based on a modified couple stress theory”, *J. Micromech. Microeng.* **16** (2006), 2355–2359.
- [Park and Gao 2008] S. K. Park and X.-L. Gao, “Variational formulation of a modified couple stress theory and its application to a simple shear problem”, *Z. Angew. Math. Phys.* **59**:5 (2008), 904–917.
- [Reddy 2007] J. N. Reddy, *Theory and analysis of elastic plates and shells*, 2nd ed., CRC, Boca Raton, FL, 2007.
- [Reddy and Jinseok 2012] J. N. Reddy and K. Jinseok, “A nonlinear modified couple stress-based third-order theory of functionally graded plates”, *Compos. Struct.* **94** (2012), 1128–1143.
- [Shu 2000] C. Shu, *Differential quadrature and its application in engineering*, Springer, London, 2000.
- [Timoshenko and Goodier 1970] S. Timoshenko and J. N. Goodier, *Theory of elasticity*, 3rd ed., McGraw-Hill, New York, 1970.
- [Toupin 1962] R. A. Toupin, “Elastic materials with couple-stresses”, *Arch. Ration. Mech. Anal.* **11**:1 (1962), 385–414.
- [Toupin 1964] R. A. Toupin, “Theories of elasticity with couple-stress”, *Arch. Ration. Mech. Anal.* **17** (1964), 85–112.
- [Tsiatas 2009] G. C. Tsiatas, “A new Kirchhoff plate model based on a modified couple stress theory”, *Int. J. Solids Struct.* **46** (2009), 2757–2764.
- [Wang et al. 2012] B. Wang, J. Zhao, and S. Zhou, “A micro scale Timoshenko beam model based on strain gradient elasticity theory”, *Eur. J. Mech. A Solids* **29** (2012), 591–599.
- [Witvrouw and Mehta 2005] A. Witvrouw and A. Mehta, “The use of functionally graded poly-SiGe layers for MEMS applications”, *Mater. Sci. Forum* **492–493** (2005), 255–260.
- [Xia et al. 2010] W. Xia, L. Wang, and L. Yin, “Nonlinear non-classical microscale beams: static bending, postbuckling and free vibration”, *Int. J. Eng. Sci.* **48**:12 (2010), 2044–2053.
- [Yang et al. 2002] F. Yang, A. C. M. Chong, D. C. C. Lam, and P. Tong, “Couple stress based strain gradient theory for elasticity”, *Int. J. Solids Struct.* **39**:10 (2002), 2731–2743.

Received 28 May 2012. Revised 26 Oct 2012. Accepted 8 Nov 2012.

REZA ANSARI: [r\\_ansari@guilan.ac.ir](mailto:r_ansari@guilan.ac.ir)

Department of Mechanical Engineering, University of Guilan, P.O. Box 3756, Rasht, Iran

MOSTAFA FAGHIH SHOJAEI: [mfsh@live.com](mailto:mfsh@live.com)

Department of Mechanical Engineering, University of Guilan, P.O. Box 3756, Rasht, Iran

VAHID MOHAMMADI: [v.n.m@live.com](mailto:v.n.m@live.com)

Department of Mechanical Engineering, University of Guilan, P.O. Box 3756, Rasht, Iran

RAHEB GHOLAMI: [rahebgholami@gmail.com](mailto:rahebgholami@gmail.com)

Department of Mechanical Engineering, University of Guilan, P.O. Box 3756, Rasht, Iran

MOHAMMAD ALI DARABI: [mad.fluid.darabi@gmail.com](mailto:mad.fluid.darabi@gmail.com)

Department of Mechanical Engineering, University of Guilan, P.O. Box 3756, Rasht, Iran

# JOURNAL OF MECHANICS OF MATERIALS AND STRUCTURES

[msp.org/jomms](http://msp.org/jomms)

Founded by Charles R. Steele and Marie-Louise Steele

## EDITORS

CHARLES R. STEELE Stanford University, USA  
DAVIDE BIGONI University of Trento, Italy  
IWONA JASIUK University of Illinois at Urbana-Champaign, USA  
YASUhide SHINDO Tohoku University, Japan

## EDITORIAL BOARD

H. D. BUI École Polytechnique, France  
J. P. CARTER University of Sydney, Australia  
R. M. CHRISTENSEN Stanford University, USA  
G. M. L. GLADWELL University of Waterloo, Canada  
D. H. HODGES Georgia Institute of Technology, USA  
J. HUTCHINSON Harvard University, USA  
C. HWU National Cheng Kung University, Taiwan  
B. L. KARIHALOO University of Wales, UK  
Y. Y. KIM Seoul National University, Republic of Korea  
Z. MROZ Academy of Science, Poland  
D. PAMPLONA Universidade Católica do Rio de Janeiro, Brazil  
M. B. RUBIN Technion, Haifa, Israel  
A. N. SHUPIKOV Ukrainian Academy of Sciences, Ukraine  
T. TARNAI University Budapest, Hungary  
F. Y. M. WAN University of California, Irvine, USA  
P. WRIGGERS Universität Hannover, Germany  
W. YANG Tsinghua University, China  
F. ZIEGLER Technische Universität Wien, Austria

**PRODUCTION** [production@msp.org](mailto:production@msp.org)

SILVIO LEVY Scientific Editor

---

See [msp.org/jomms](http://msp.org/jomms) for submission guidelines.


---

JoMMS (ISSN 1559-3959) at Mathematical Sciences Publishers, 798 Evans Hall #6840, c/o University of California, Berkeley, CA 94720-3840, is published in 10 issues a year. The subscription price for 2012 is US \$555/year for the electronic version, and \$735/year (+\$60, if shipping outside the US) for print and electronic. Subscriptions, requests for back issues, and changes of address should be sent to MSP.

---

JoMMS peer-review and production is managed by EditFlow® from Mathematical Sciences Publishers.

PUBLISHED BY

 **mathematical sciences publishers**  
nonprofit scientific publishing

<http://msp.org/>

© 2012 Mathematical Sciences Publishers

- Indentation and residual stress in the axially symmetric elastoplastic contact problem** TIAN-HU HAO 887
- Form finding of tensegrity structures using finite elements and mathematical programming** KATALIN K. KLINKA, VINICIUS F. ARCARO and DARIO GASPARINI 899
- Experimental and analytical investigation of the behavior of diaphragm-through joints of concrete-filled tubular columns** RONG BIN, CHEN ZHIHUA, ZHANG RUOYU, APOSTOLOS FAFITIS and YANG NAN 909
- Buckling and postbuckling behavior of functionally graded Timoshenko microbeams based on the strain gradient theory** REZA ANSARI, MOSTAFA FAGHIH SHOJAEI, VAHID MOHAMMADI, RAHEB GHOLAMI and MOHAMMAD ALI DARABI 931
- Measurement of elastic properties of AISI 52100 alloy steel by ultrasonic nondestructive methods** MOHAMMAD HAMIDNIA and FARHANG HONARVAR 951
- Boundary integral equation for notch problems in an elastic half-plane based on Green's function method** Y. Z. CHEN 963
- Internal structures and internal variables in solids** JÜRI ENGELBRECHT and ARKADI BEREZOVSKI 983
- The inverse problem of seismic fault determination using part time measurements** HUY DUONG BUI, ANDREI CONSTANTINESCU and HUBERT MAIGRE 997